Tropical Cyclone– and Monsoon-Induced Rainfall Variability in Taiwan

JAU-MING CHEN

Institute of Navigation Science and Technology, National Kaohsiung Marine University, Kaohsiung, Taiwan

TIM LI

International Pacific Research Center, University of Hawaii at Manoa, Honolulu, Hawaii

CHING-FENG SHIH

Research and Development Center, Central Weather Bureau, Taipei, Taiwan

(Manuscript received 24 July 2009, in final form 15 March 2010)

ABSTRACT

This study investigates the interannual variability of tropical cyclone (TC)- and monsoon-induced rainfall (P) in Taiwan during July–September for the period 1950–2002. To examine the relative effects of TCs and monsoons, local rainfall in Taiwan is separated into two subcomponents: TC rainfall (P_{TC}) and seasonal monsoon rainfall (P_{SM}). The former is induced by TC passage across Taiwan, while the later is caused by large-scale monsoon circulation.

Climatologically, P_{TC} and P_{SM} accounts for 47.5% and 52.5% of total rainfall in Taiwan, respectively, showing a comparable contribution. On an interannual time scale, P_{TC} and P_{SM} anomalies tend to vary inversely. Two dominant rainfall variability types are found in Taiwan: enhanced P_{TC} but suppressed P_{SM} (T+S−) and suppressed P_{TC} but enhanced P_{SM} (T−S+). The T+S− type features a low-level anomalous cyclone and enhanced upward motion southeast of Taiwan. This favorable environmental condition leads to more TC formation in the region. TCs are further steered by mean southeasterly flows toward Taiwan to increase P_{TC} (T+). As Taiwan is located in the western boundary of the anomalous cyclone, anomalous northeasterly water vapor fluxes hinder moisture supplies from the South China Sea into Taiwan, resulting in decreased P_{SM} (S−). The T−S+ type concurs with an anomalous cyclone over Taiwan. Its center enhances upward motion and moisture fluxes from the South China Sea into Taiwan, yielding increased P_{SM} (S+). Meanwhile, weak relative vorticity anomalies occur to the southeast of Taiwan, suppressing TC formation in the region. Mean southerly steering flows tend to drive more TCs toward Japan and the North Pacific, resulting in decreased TC frequency and P_{TC} in Taiwan (T−).

The present approach provides a new perspective for studying and predicting interannual rainfall variability via the separation of rainfall into TC- and monsoon-induced rainfall subcomponents, rather than looking solely at total rainfall. The result shows that there are two ways to significantly increase total rainfall in Taiwan (T+S− and T−S+), but there is only one way to decrease it (T−S−). The composites of circulation anomalies based on two rainfall indexes have more significant and coherent dynamic patterns than those sorted based on the total rainfall index.

1. Introduction

The major rain-bearing systems in the conjunction regions between the Asian continent and the western North Pacific (WNP) include monsoon-related frontal systems and tropical cyclone (TC) activity. Climatologically, monsoon rainbands first appear in the South China Sea (SCS) in mid-May, move northward during June and July in concurrence with the formation of the East Asian (EA) monsoon frontal systems over China, Japan, and Korea, and later shift to the tropical WNP–Philippine Sea region in August (e.g., Chen 1994; Ding 1994; Wang 1994; Chang and Chen 1995; Chen and Chen 1995; Kang et al. 1999; Lim et al. 2002; Wu 2002; see Li and Wang 2005 for a review). These rainfall activities normally last for a month or longer, integrating into an Asian–Pacific monsoon from May to September (Wang and LinHo 2002). A tropical cyclone

Corresponding author address: Jau-Ming Chen, Institute of Navigation Science and Technology, National Kaohsiung Marine University, No. 482, Jhongjhou 3rd Rd., Kaohsiung, 805, Taiwan.
E-mail: cjming@mail.nkmu.edu.tw

DOI: 10.1175/2010JCLI3355.1

(TC)'s life cycle ranges from 1 to 2 weeks, being transient in nature (e.g., Wang and Chan 2002). TC activity worldwide is most intense over the WNP region, where most TCs form inside or nearby the monsoon trough (MT; e.g., McBride 1995). After formation, a TC may follow a westward track toward Asia or recurve northward toward the North Pacific (Harr and Elsberry 1991).

Both the monsoon rainfall and the TC activity are greatly modulated by the Madden–Julian oscillation (MJO; Madden and Julian 1971). A number of studies showed that the MJO can modulate TC formation over the southern Indian Ocean, the Australian region (south of equator; 105-160° E), and the WNP (e.g., Liebmann et al. 1994; Hall et al. 2001; Bessafi and Wheller 2006; Fu et al. 2007; Kim et al. 2008). An increase of TC genesis frequency often concurs with an active MJO phase over the WNP and the northeast of Australia. The eastward propagation of the MJO may trigger a meridionally propagating intraseasonal oscillation (ISO; e.g., Li and Wang 1994; Wang and Xie 1997; Jiang et al. 2004; Hsu 2005). Over the WNP, the westerly (easterly) phase of an ISO corresponds to a deepened MT [an intensified Pacific subtropical high (PSH)]. As a consequence, TCs in the regions tend to have a recurving (straight moving) track (e.g., Ko and Hsu 2009; Chen et al. 2009). The northward-propagating ISO plays an important role in promoting the intraseasonal monsoon variability over South Asia, East Asia, and the SCS (e.g., Chen and Chen 1995; Wu et al. 1999; Mao and Chan 2005; Hoyos and Webster 2007; Krishnamurthy and Shukla 2007). The EA monsoon rainband exhibits a stepwise progression feature, with a maximum rainband over southern China in May, a mei-yu front over central China in June, and polar frontal rains over northeastern China in July (e.g., Lau et al. 1988; Li and Wang 2005).

The WNP TC activity and monsoon also undergo a noticeable interannual variability. Both the local sea surface temperature (SST) anomalies and remote forcing of the El Niño–Southern Oscillation, tropical Indian Ocean, and Antarctic Oscillation play important roles in determining the interannual variability of the MT and PSH (e.g., Chan 2000; Chia and Ropelewski 2002; Wang et al. 2003; Chou et al. 2003; Yoo et al. 2004; Wang and Li 2004; Ho et al. 2005; Kim et al. 2005; Sui et al. 2007; Wu et al. 2009, 2010). SST and convection anomalies over the SCS–Philippine Sea regions induce a prominent meridional wave train over East Asia and the WNP, affecting the PSH and MT (e.g., Wang and Fan 1999; Lu 2001) and leading to meridionally stratified rainfall patterns in China (e.g., Huang and Wu 1989; Liu and Ding 1992; Wang et al. 2001). Chen et al. (2010) found that a strong eastward (westward) displacement in both the PSH and MT corresponds to a low-level anomalous cyclone (anticyclone) centering near Taiwan and a significant increase (decrease) in the local mei-yu rainfall. The eastward-displacing MT concurs with the intensification and eastward extension of equatorial westerlies over the western Pacific (e.g., Lander 1994), followed by an eastward shift in TC formation location and the subsequent TC activity (e.g., Chen et al. 1998; Chan 2000; Wang and Chan 2002; Wang and Zhang 2002). During the decaying phase of an El Niño, the monsoon rainfall along the mei-yu front tends to be wet because of the intensification of pressure gradients to the northwest of a low-level anomalous Philippine Sea anticyclone (e.g., Wang et al. 2000, 2003; J.-M. Chen et al. 2007) and the increase of moisture transports from the SCS into East Asia by its outer flows (e.g., Chang et al. 2000a,b). On the other hand, this anomalous anticyclone hinders large-scale ascending motion over the tropical western Pacific, leading to suppressed TC activity and TC rainfall over the WNP and EA regions (e.g., Chan 2000).

The works listed earlier reveal an interesting phenomenon: enhanced monsoon rainfall and suppressed TC activity may concur over the WNP and EA regions. This suggests that rainfall components induced by transient TC activity and seasonal monsoon climate may contribute oppositely to total EA rainfall, leading to its complex interannual variability. However, the relative role of these two components in the interannual variability of the EA rainfall has not been comprehensively examined. This is partially because total rainfall, instead of rainfall subcomponents, is broadly used as the analysis index for monsoon-related studies (e.g., Parthasarathy et al. 1992; Wang and LinHo 2002). The main purpose of this study is to specifically examine how monsoon and TC activity jointly modulate the interannual variability of the EA rainfall. Rainfall variability in Taiwan is taken as the case for analysis in this study. As shown in Fig. 1, Taiwan is an island off the southeastern coasts of the Asian continent, with the EA summer monsoon to its north and the WNP summer monsoon to its south (e.g., Wang and LinHo 2002). It is also situated in the overlapping zone of the westward-moving and northward-recurving TC tracks (e.g., Ho et al. 2004; Chen et al. 2005). TC activity and monsoon processes make up two of the most important rainfall mechanisms during the major rainy seasons of Taiwan (e.g., Chen and Fan 2003). The key questions raised in this study are as follows:

- Climatologically, what are the relative contributions of rainfall subcomponents associated with monsoon and TC activity to total rainfall for Taiwan?
- On an interannual time scale, what are the major rainfall variability types induced by monsoon and TC

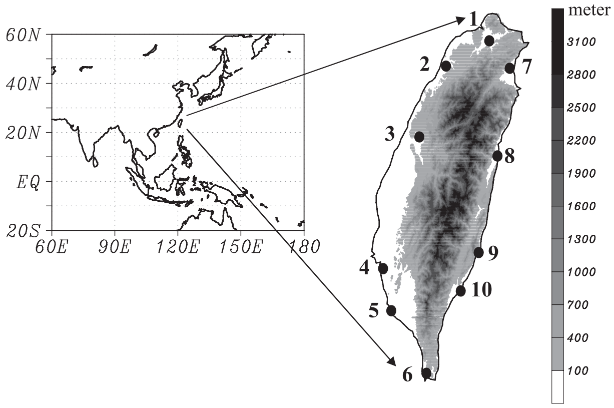

FIG. 1. The geographical distributions of Taiwan and its topography, and 10 major meteorological stations around this island.

TABLE 1. Detailed information about the 10 stations in Taiwan shown in Fig. 1.

No.	Station	Longitude	Latitude	Altitude(m)
1	Taipei	121°30′24″	25°02′23″	5.3
2	Hsinchu	121°00′22″	24°49′48″	34.0
3	Taichung	120°40′33″	24°08′51″	34.0
4	Tainan	120°13′43″	23°02′22″	8.1
5	Kaohsiung	120°18′29″	22°34′04″	2.3
6	Hengchun	120°44′17″	22°00′20″	22.1
7	Ilan	121°44′53″	24°45′56″	7.2
8	Hualian	121°36′18″	23°58′37″	16.0
9	Chengkuan	121°21′55″	23°05′57″	33.5
10	Taitung	121°08′48″	22°45′15″	9.0

activity for Taiwan? What are the corresponding large-scale processes regulating rainfall variability?

- Does the present approach of analyzing rainfall by two major subcomponents help us to better understand interannual rainfall variability as compared with the conventional approach of using total rainfall as an index?

The objective of the present study is to provide more detailed understandings of the regulating processes that control interannual rainfall variability in the EA and WNP monsoon regions. Improved understandings may help enhance our knowledge about the dynamics of rainfall variability in the region and advance seasonal climate prediction.

2. Data

This study analyzes four datasets. The first set includes daily rainfall records from 10 major meteorological stations in Taiwan (Fig. 1). They are used to depict rainfall variability in Taiwan caused by TC activity and monsoon climate. Detailed information about these 10 stations is listed in Table 1. The second set is the National Centers for Environmental Prediction–National Center for Atmospheric Research (NCEP–NCAR) reanalysis (Kalnay et al. 1996), which is hereafter referred to as the reanalysis data. The monthly reanalysis data are used to reveal large-scale circulation patterns associated with interannual rainfall variability. The third set is the monthly precipitation of the Climate Prediction Center (CPC) Merged Analysis of Precipitation (CMAP) data for the period 1980–2002 (Xie and Arkin 1997). They are employed to portray the climatological pattern of summer rainfall over the Asian–Pacific region (Fig. 2b). The fourth set is the 6-h WNP TC best-track data from the Joint Typhoon Warning Center (JTWC). The JTWC archives include data from 1945 onward. Efforts were made to correct the discrepancies and inhomogeneity of this dataset, particularly for the WNP region during the period 1950–2000 (e.g., Chu et al. 2002). To consider the data quality of the WNP best-track data, the analysis period in this study spans from 1950 to 2002.

3. Major rainy seasons in Taiwan

The monsoon system persists in the Asian–Pacific region from May to September (e.g., Wang and LinHo 2002). During this period, TC activity exhibits rather distinct intensity in Taiwan. According to official statistics of the Central Weather Bureau, Taiwan, for the twentieth century, of the TCs affecting Taiwan, 23.3% occur in July, 29.3% in August, 22.6% in September, 3.8% in May, and 7.9% in June. The major rainy seasons in Taiwan are conventionally divided into the TC-inactive-but-monsoon-active May–June period and the active-monsoon-and-active-TC July–September period (e.g., Chen 1994; Chen and Yu 1988; Hsu et al. 2005). To examine prominent effects from both TC and monsoon activity on local rainfall in Taiwan, the July–September period is analyzed.

The climatological (1950–2002) states of monsoon and TC activity for July–September over the Asian–Pacific region are shown in Fig. 2. The low-level monsoon circulation (Fig. 2a), represented by the reanalysis 850-hPa streamfunction (*S*850), is recognized by the PSH to the east, Asian continental low to the west, and MT to the southeast stretching from the SCS into the tropical WNP region. The 10-m winds of the reanalysis data and the CMAP precipitation (Fig. 2b) indicate that southwesterly flows prevail over the Arabian Sea, the Bay of Bengal, and the SCS to maintain major rainbands over these areas. Elongated rainbands occur in the WNP MT region, where TC activity is rigorous. Using the 6-h records of the JTWC best-track data, TC frequency is measured by the total count of TC appearance in every 3° × 3° box throughout July–September. TC activity analyzed in this study includes both tropical storms and typhoons with maximum

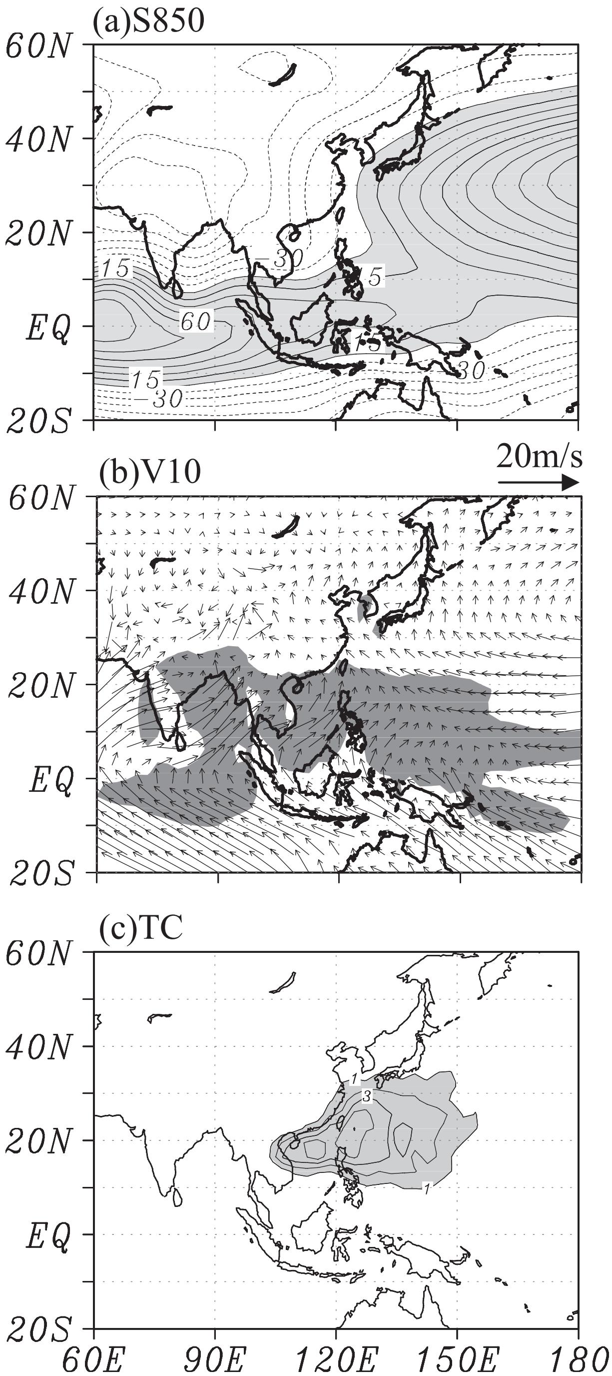

FIG. 2. The 1950–2002 climatological states for July–September: (a) the low-level circulation represented by 850-hPa streamfunction, (b) 10-m winds (vector) and precipitation (shading), and (c) TC frequency represented by the total number of TC observations throughout the period. In (a), contour intervals are 15×10^5 m^2 s^{-1}, and positive values are shaded. In (b), precipitation larger than 7 mm day^{-1} is shaded. In (c), contour intervals are 1, and values larger than 1 are shaded.

sustained wind speeds exceeding 34 kt. The climatological pattern of TC frequency (Fig. 2c) reveals two major tracks emanating from the tropical western Pacific: a westward straight track toward the SCS and a northward-recurving track toward Japan and the North Pacific. This pattern indicates that rainbands over the tropical western Pacific are closely associated with energetic TC activity.

Summer rainfall in Taiwan is primarily influenced by monsoon southwesterly flows originating from the SCS and TC passages from the western Pacific. Therefore, summer rainfall in Taiwan is generally categorized into two major subcomponents: TC rainfall and non-TC rainfall (e.g., Chen and Chen 2003; Chen et al. 2005). The former is a transient process, caused by a TC's passage through the vicinity of Taiwan. The latter is a season-integrating process, with a major contribution from rainstorms associated with the monsoon southwesterly flows interacting with local topography and a minor contribution from fronts, land breeze, and other rainfall events without a distinct weather system (e.g., Chen and Chen 2003; Wang and Chen 2008). Since the non-TC rainfall is, in general, connected to the background monsoon climate, it is referred to as seasonal monsoon rainfall in this study. TC rainfall is commonly interpreted as rainfall occurring within a spatial range from the TC center; however, so far, no consensus has been reached with respect to the range (e.g., Chen et al. 2005; C.-S. Chen et al. 2007; Jiang and Zipser 2010; Kubota and Wang 2009). Given that the major rainbands of a TC are normally confined in a region of 200–300-km radius from the TC center, a distance of 2.5° in longitude and latitude (approximately 250 km) should be capable of capturing the majority of TC rainfall. Chen et al. (2005) used this definition to study the interannual variability of TC rainfall over Taiwan and found its coherent connection to background large-scale processes.

With these considerations in mind, we conduct the following rainfall categorizations. When a TC has its center in a region close to Taiwan within 2.5° in longitude and latitude (19.5°–27.5°N, 117.5°–124.5°E), rainfall induced by the TC's surrounding flows in Taiwan during these days is categorized as TC rainfall (P_{TC}). Other than TC rainfall, the remaining contribution to July–September rainfall is primarily associated with monsoon southwesterly flows interacting with local topography and the diurnal cycle. For simplicity, the remaining rainfall part is referred to as seasonal monsoon rainfall (P_{SM}). The climatological means of total P_{TC} and P_{SM} for the 10 major stations in Taiwan are shown in Fig. 3. In general, P_{SM} is greater than P_{TC} over western Taiwan, while P_{TC} is greater than P_{SM} over eastern Taiwan. This is because western Taiwan is at the windward side of the southwesterly monsoon flows, while eastern Taiwan

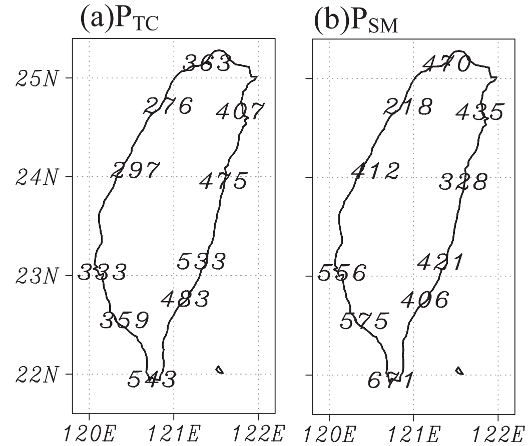

FIG. 3. The 1950–2002 climatology of rainfall subcomponents accumulated throughout July–September in the 10 major stations over Taiwan: (a) TC rainfall and (b) seasonal monsoon rainfall; unit: mm.

is at the windward side of TC passage from the western Pacific. A peculiar feature is that P_{SM} is particularly low at Hsinchu (station 2) over western Taiwan. Liu (1996) suggested that the suppressed convective activity over Hsinchu is possibly attributed to the effect of local topography interacting with large-scale flows. The 10-station rainfall average is 407 mm for P_{TC} and 449 mm for P_{SM}. Subcomponents P_{TC} and P_{SM} account for 47.5% and 52.5% of total rainfall, respectively. These two rainfall subcomponents contribute comparably to total July–September rainfall in Taiwan.

4. Interannual rainfall variability

The relative effects of the monsoon and TC on interannual rainfall variability in Taiwan are examined from the 1950–2002 time series of July–September P_{SM} and P_{TC} averaged from 10 major stations (Fig. 4). The standard deviation (SD) of the P_{SM} time series is 163 mm and 216 mm for the P_{TC} time series. Here P_{TC} has a smaller climatological mean—but a much larger SD—than P_{SM}. Moreover, the P_{SM} and P_{TC} time series tend to fluctuate inversely with a simultaneous correlation coefficient of -0.46. The P_{SM}–P_{TC} correlation reaches a maximum at zero lag. The major types of interannual rainfall variability in Taiwan jointly induced by monsoon and TC activity are categorized by the following criteria: both P_{TC} and P_{SM} anomalies in that year have to exceed 0.7 SD (equivalent to 151 mm for P_{TC} and 114 mm for P_{SM}). A standard deviation of 0.7, instead of 1 SD, is used because temporal and spatial features of regional-scale rainfall variability in Taiwan are more chaotic than those of the large-scale variability phenomenon (e.g., Chen et al. 2005; Chen et al. 2008; Chen et al. 2010). Moreover, the use of dual

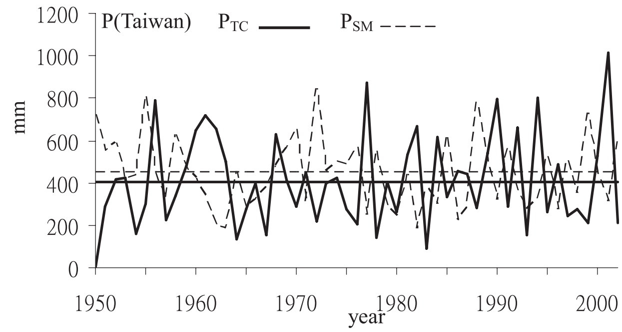

FIG. 4. The 1950–2002 time series of P_{TC} and P_{SM} averaged from 10 major stations in Taiwan.

indexes—P_{SM} and P_{TC}—leads to more variability types and correspondingly fewer samples in each type. To increase the number of composite cases in the major variability types, it is necessary to lower the categorization criterion to some extent.

The selection results in three variability types in Table 2: 1) enhanced P_{TC} but suppressed P_{SM} (denoted as T+S− type), 2) suppressed P_{TC} but enhanced P_{SM} (denoted as T−S+ type), and 3) suppressed P_{TC} and P_{SM} (denoted as T−S− type). There are 7 yr in the T+S− type, 6 yr in the T−S+ type, only 2 yr in the T−S− type. The T−S− type is excluded from analysis because of the lack of sufficient case numbers. It is interesting to note that no

TABLE 2. Major rainfall variability types in Taiwan during the July-September season categorized by TC rainfall (P_{TC}) and seasonal monsoon rainfall (P_{SM}): the member years, anomalies of P_{TC}, P_{SM}, and *S*850, and type names. Increased and decreased P_{TC} is denoted as the T+ and T− types, respectively, while the S+ and S- types represent for increased and decreased P_{SM}, respectively. C and AC represent for anomalous cyclone and anticyclone, respectively. Averages of each type are listed.

Year	P_{TC}	P_{SM}	*S*850 anomaly	Type
1961	313	~118	C	T+S−
1977	467	~199	C	
1982	260	~262	C	
1984	208	~149	C	
1990	389	~127	C	
1994	397	~119	C	
2001	609	~134	C	
AVG	**378**	**−158**		
1950	~407	274	C	T−S+
1978	~265	115	C	
1972	~187	395	C	
1976	~202	123	C	
1999	~193	282	C	
2002	~193	145	C	
AVG	**−241**	**222**		
1957	~182	~119	AC	T−S−
1993	~256	~176	AC	
AVG	**−219**	**−148**		

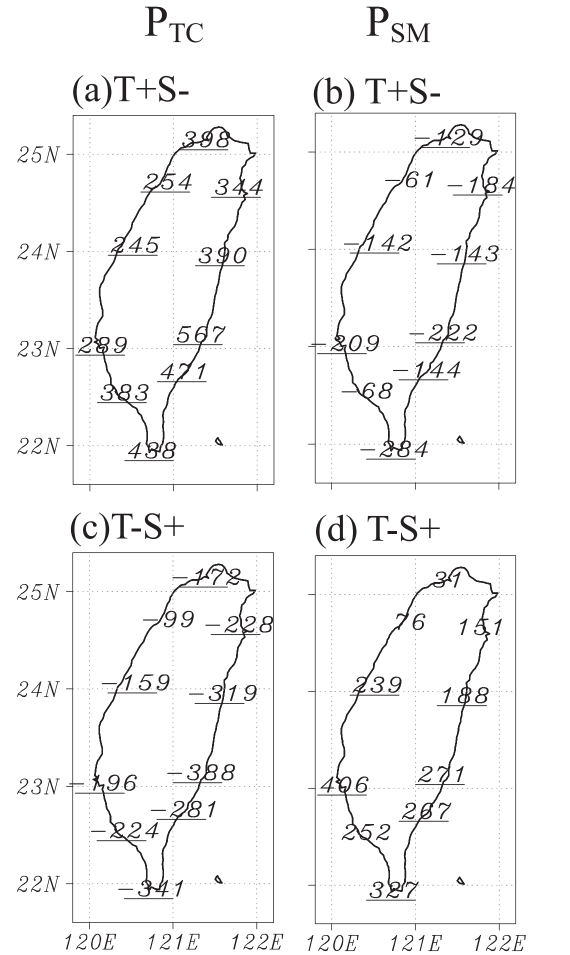

FIG. 5. Composite anomalies of (left) P_{TC} and (right) P_{SM} in Taiwan for the T+S− and T−S+ types. Composite anomalies significant at the 95% level are underlined.

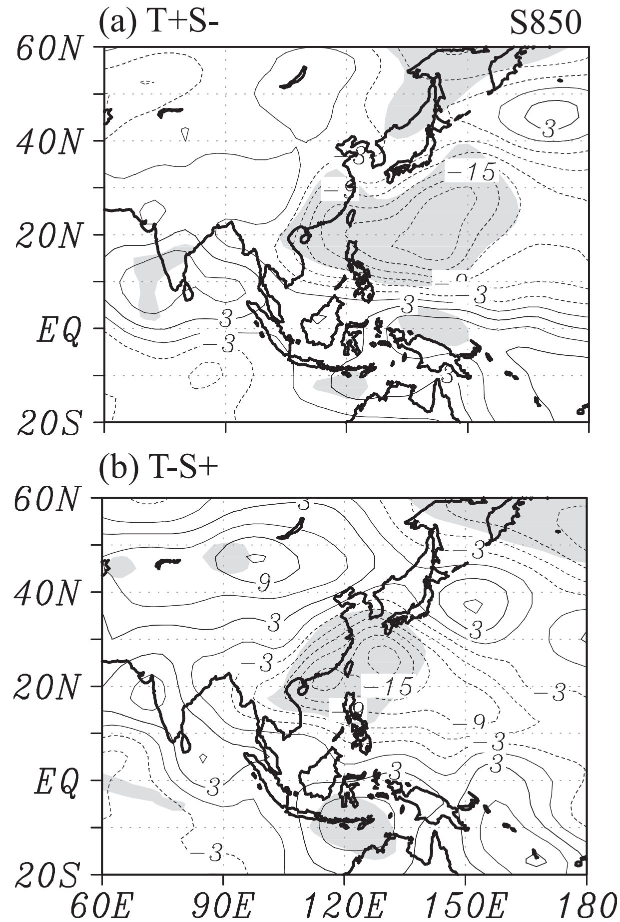

FIG. 6. Composite anomalies of the low-level circulation represented by $S850$ for the (a) T+S− type and (b) T−S+ type. Contour intervals are 3×10^5 m^2 s^{-1}, and anomalies significant at the 95% level are shaded.

T+S+ case is found. The dominance of the T+S− and T−S+ types indicates that monsoons and TCs tend to exert opposite influences on local rainfall variability in Taiwan, consistent with the negative P_{TC}–P_{SM} correlation coefficient. Further analyses reveal that the majority of stations (six or more) exhibit the same anomalous sign as the area-average values for both P_{TC} and P_{SM} anomalies in each member year of the T+S− and T−S+ types. As such, it is reasonable to use the area-average values to represent the gross variability features of P_{TC} and P_{SM} over the Taiwan region. This study focuses on comparing rainfall processes between the T+S− and T−S+ types.

Composite P_{TC} and P_{SM} anomalies in Taiwan for the T+S− and T−S+ types are illustrated in Fig. 5. Anomalies significant at the 95% level of the Student's *t* test are underlined. In general, P_{TC} and P_{SM} anomalies are significant at 6 or more out of 10 stations in each type. These anomalies exhibit a uniform sign throughout all the stations. An island-wide pattern in Taiwan implicates a close connection between its local climate anomalies and large-scale background variations—in particular, the low-level circulation anomaly (e.g., Hsu and Chen 2002; Hung et al. 2004; Chen et al. 2005). Differences in large-scale regulatory processes between these two types need to be explored.

5. The monsoon-regulating processes

The regulating processes through which the low-level monsoon circulation affects rainfall in Taiwan are analyzed in terms of composite $S850$ anomalies (Fig. 6). The common and significant feature for both T+S− and T−S+ types is an anomalous cyclone overlying Taiwan, but with different spatial distributions. The anomalous cyclone center appears to the southeast of Taiwan in the T+S− type, but it extends from the southwest to the northeast across Taiwan in the T−S+ type. Taiwan is located in the western boundary of the anomalous

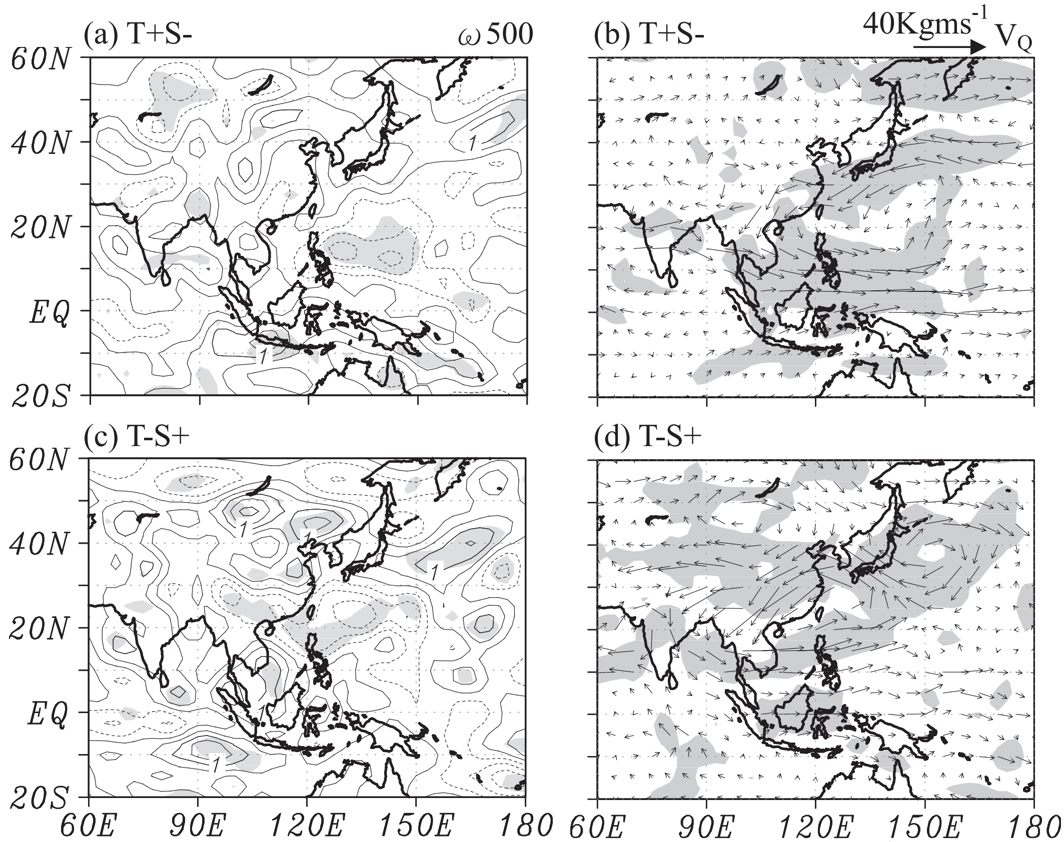

FIG. 7. As in Fig. 6, but for composite anomalies of (left) 500-hPa vertical motion and (right) vertically integrated moisture flux for the T+S− and T−S+ types. Contour intervals are 0.5×10^{-4} mb s^{-1} in (a) and (c). Composite anomalies significant at the 95% level are shaded.

cyclone in the T+S− type, but it is near the center in the T−S+ type. An examination of the *S*850 pattern for each individual member further confirms the features mentioned earlier. Taiwan is affected by anomalous flows from the north (1961, 1982), northeast (1977, 1984, 1994, 2001), or southeast (1990) in the T+S− type. These anomalous flows from the north and the east tend to weaken the mean southwesterly flows from the SCS, corresponding to a decreased P_{SM} (S−). For the T−S+ type, Taiwan is influenced by anomalous flows from the southwest (1950, 1972, 1999, 2002) or south (1976, 1978). These anomalous flows tend to enhance southwesterly flows into Taiwan, leading to an increased P_{SM} (S+).

There are two major mechanisms for the anomalous low-level circulation to affect monsoon-related rainfall in Taiwan: vertical motion around its central region and moisture transport by its surrounding flows (e.g., Jiang et al. 2003; Chen et al. 2005; Chen et al. 2008). To delineate these two mechanisms, composite anomalies of 500-hPa vertical motion (ω500) and moisture transport ($\mathbf{V}_Q$) are illustrated in Fig. 7. Moisture transport is depicted by a vertically integrated water vapor flux, $\mathbf{V}_Q = \int_p^{p_0} \mathbf{V} q\, dp$, where $\mathbf{V}$ is the horizontal wind vector, q is the specific humidity, and the vertical integral is from a given pressure level to $p_0 = 1000$ hPa. Note that the ω500 anomaly over Taiwan is insignificant and weak with near-zero intensity in the T+S− type (Fig. 7a); however, it exhibits significant upward motion (negative value) to facilitate P_{SM} in the T−S+ type (Fig. 7c). The $\mathbf{V}_Q$ anomaly in the T+S− type (Fig. 7b) influences Taiwan via anomalous northeasterly fluxes induced by outer flows over the western boundary of the anomalous cyclone. These anomalous fluxes hinder the entrance of water vapor fluxes from the SCS into Taiwan, leading to decreased P_{SM} in Taiwan. For the T−S+ type (Fig. 7d), the $\mathbf{V}_Q$ anomaly associated with the anomalous cyclone center to the southwest of Taiwan enhances the water vapor fluxes from the SCS, leading to increased P_{SM} over Taiwan. A detailed examination of the $\mathbf{V}_Q$ anomaly for each member (not shown) reveals that anomalous moisture transport is from the northeast or north in the T+S− type but from the southwest or south in the T−S+ type. As a result, total southwesterly moisture transport appears to be weakened in the former but enhanced in

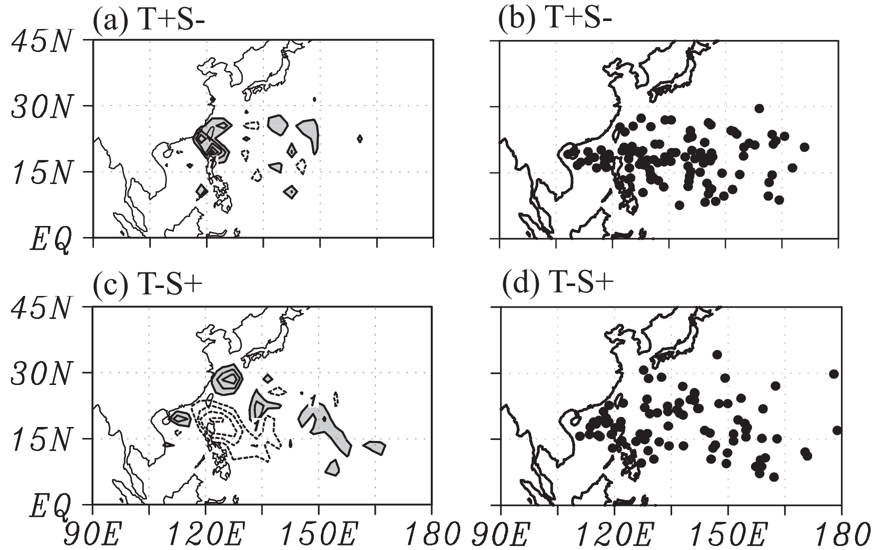

FIG. 8. Composite patterns of (a),(c) accumulated TC frequency anomalies in every 3° × 3° box and (b),(d) TC formation location throughout July–September for the T+S−/T−S+ type. In (a) and (c), contour intervals are 1 and the contour of zero is suppressed. Positive values are shaded.

the latter. In brief, a decreased P_{SM} in the T+S− type results from anomalous weak vertical motion over Taiwan and suppressed moisture supplies of the southwesterly flows from the SCS into Taiwan. On the other hand, anomalous upward motion and intensified moisture supplies by the southwesterly flows enhance P_{SM} in the T−S+ type. The categorization of S+ and S− types is evidently connected to local anomalous moisture transport associated with the variability of southwesterly flows; therefore, it can be considered to well represent monsoon-related rainfall variability.

6. Factors affecting TC activity

Circulation variability may regulate both TC frequency and track in the WNP (e.g., Wang and Chan 2002; Chen et al. 2005). Composite patterns of TC frequency (estimated in the same way as the climatology shown in Fig. 2c) anomalies and TC formation location for the two rainfall variability types are shown in Fig. 8. As shown in Fig. 8a (Fig. 8c), TC frequency increases (decreases) in the vicinity of Taiwan in the T+S− (T−S+) type, corresponding to increased (decreased) P_{TC}. For both types, TC frequency anomalies over Taiwan originate from its southeastern regions. The oceanic regions southeast of Taiwan—that is, 0°–21°N, 120°–150°E—are thus referred to as the TC formation zone. As revealed by Figs. 8b and 8d, more TCs form in the TC formation zone in the T+S− type than the T−S+ type, particularly in the regions immediately to the southeast of Taiwan (i.e., 10°–20°N, 120°–135°E). In fact, the composite number of TC formation in the TC formation zone is 6.9 in the T+S− type and 3.5 in the T−S+ type, and the climatological mean value is 6.1. For the T−S+ type, TCs tend to form in a more northward region, specifically to the east and northeast of Taiwan. The spatial difference is possibly attributed to the asymmetry of spatial distributions of large-scale environmental flows that regulate TC formation. The asymmetry can be clearly seen from 850-hPa relative vorticity (ζ850; Fig. 9) and vertical motion (Fig. 7) fields. Over the TC formation zone, the increased (decreased) TC frequency in the T+S− (T−S+) type is concurrent with significant positive (much weaker) ζ850 anomalies there. For the T−S+ type, significant positive ζ850 anomalies appear in the regions northeast of Taiwan, coherent with more TC formation there. A further diagnosis reveals that the ζ850 anomalies in both types are mainly contributed to by the meridional shear of zonal wind (i.e., $-\partial u/\partial y$), and that they are spatially coherent with the centers of S850 anomalies (see Fig. 6). The vertical motion anomalies exhibit a spatial feature resembling the ζ850 anomalies. In the TC formation zone, significant upward motion anomalies occur in the T+S− type (see Fig. 7a); however, weak and downward motion anomalies appear in the T−S+ type (see Fig. 7c). The major ascending motion anomaly in the T−S+ type shifts northward into the regions east of Taiwan.

In addition to TC formation, the TC track also determines TC frequency in Taiwan. The TC track is known to be evidently guided by a steering flow averaged vertically from 850 to 400 hPa (e.g., Gross 1991). Figure 10 illustrates the vertically integrated steering flow in the

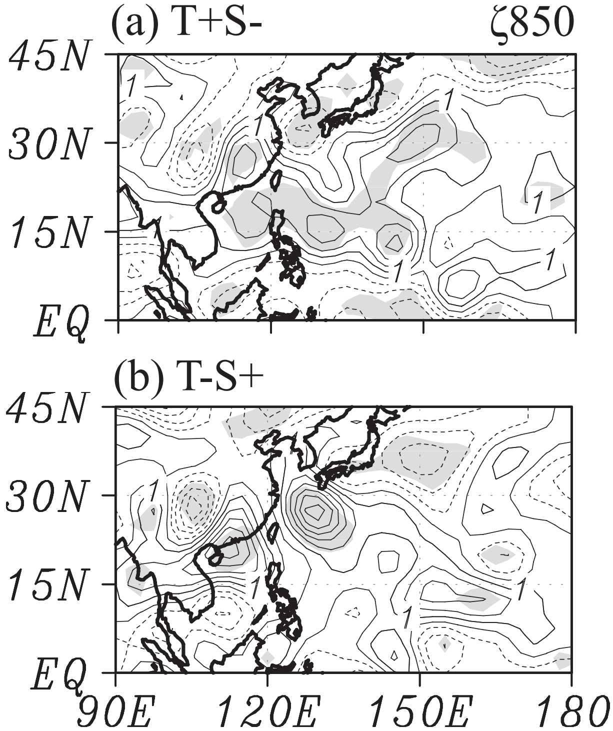

FIG. 9. As in Fig. 6, but for composite anomalies of 850-hPa relative vorticity. Contour intervals are 1×10^{-5} s^{-1}. Composite anomalies significant at the 95% level are shaded.

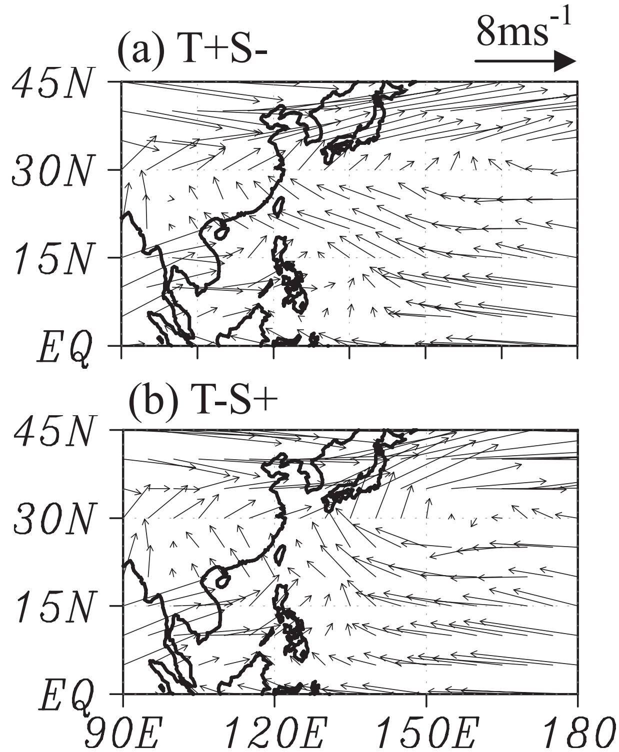

FIG. 10. Composite mean winds averaged from 850 to 400 hPa to represent steering flows for the two rainfall variability types.

WNP. The T+S− type exhibits dominant southeasterly direction steering flows to pass Taiwan. These flows certainly help to steer TCs from the formation zone toward Taiwan, resulting in increased TC frequency. On the other hand, the prevailing steering flows in the T−S+ type become more southerly in the TC formation zone. They tend to guide TCs to move northward toward Japan and the North Pacific, rather than Taiwan; thus, TC frequency in Taiwan decreases. The appearance of an anomalous cyclone center to the northeast of Taiwan (see Fig. 6b) reflects an evidently weakening or eastward retreat of the PSH. This eastward retreat adjusts mean flows over its western boundary from southeasterlies to southerlies.

These analyses disclose that more TCs are formed over the TC formation zone in the T+S− type due to the existence of strong positive low-level relative vorticity and upward motion anomalies in concurrence with an anomalous *S*850 cyclone southeast of Taiwan. These TCs are further guided by mean southeasterly steering flows toward Taiwan, yielding an increase in TC rainfall. For the T−S+ type, the anomalous cyclone center displaces northwestward. Following this displacement, relative vorticity and vertical motion anomalies become weak in the TC formation zone to hinder TC formation. Also, mean steering flows become more southerly to guide TCs moving northward from the TC formation zone into Japan and the North Pacific, thus TC rainfall in Taiwan decreases. The result is consistent with Harr and Elsberry (1995), who found that the WNP TC tracks show two types: recurve south and recurve north. The former features a low-level anomalous cyclone centering in the regions southeast of Taiwan, consistent with more TC formation there. The latter is characterized by an anomalous cyclone center and more TC formation northeast of Taiwan. In general, the T+S− type exhibits features resembling the recurve-south type, while the T−S+ type resembles the recurve-north type.

7. Comparison with total rainfall analysis

This study uses dual indexes P_{TC} and P_{SM} to delineate interannual rainfall variability. Does this approach disclose more insights into interannual rainfall variability than the conventional approach using the single index of total rainfall? To address this question, an analysis of total rainfall is conducted for comparison. The July–September total rainfall averaged from 10 major stations in Taiwan for the period 1950–2002 has a mean of 856 mm and a SD of 207 mm. By taking one SD as the threshold, anomalous wet and dry years are selected in Table 3. There are 10 anomalous wet years and nine anomalous dry years, which are denoted as the TR+ and

TABLE 3. Major variability types of total rainfall in Taiwan during the July-September season: the member years, anomalies of total rainfall (P), TC rainfall (P_{TC}), seasonal monsoon rainfall (P_{SM}), and S850, and type names. C and AC represent for anomalous cyclone and anticyclone, respectively. Increased (decreased) total rainfall is denoted as the TR+ (TR−) type.

Year	P	P_{TC}	P_{SM}	S850 anomaly	Type
1960	212	240	~28	AC	TR+
1968	254	221	33	C	
1990	262	389	~127	C	
1977	268	467	~199	C	
1994	278	397	~119	C	
1994	278	397	~119	C	
1956	386	384	2	AC	
2001	475	609	~134	C	
1988	206	~127	333	AC	
1972	208	~187	395	C	
1955	262	~106	368	AC	
AVG	**281**	**229**	**52**		
1993	~432	~256	~176	AC	TR−
1980	~352	~146	~206	AC	
1957	~301	~182	~119	AC	
1983	~390	~318	~72	AC	
1967	~329	~256	~73	AC	
1964	~265	~273	8	AC	
1954	~257	~245	~12	AC	
1965	~297	~128	~169	AC	
1998	~226	~129	~97	AC	
AVG	**−317**	**−215**	**−102**		

TR− types, respectively. The P_{TC} and P_{SM} anomalies in the TR+ type tend to have an opposite sign. Increases in the total rainfall are mainly attributed to P_{TC} in 7 yr but to P_{SM} in 3 yr. The years of 1977, 1990, 1994, and 2001 belong to the T+S− type, while the years of 1955, 1972, and 1988 have features of the T−S+ type. The TR+ type is a mixture of the T+S− and T−S+ types. As such, analyses of total rainfall cannot identify the existence of the T+S− and T−S+ types, not to mention their distinct features associated with the variability of large-scale monsoon circulation and the WNP TC activity. It is clear that analyses of rainfall subcomponents in this study are able to obtain more insights into interannual rainfall variability in the EA region than total rainfall analyses. For the TR− cases, their P_{TC} and P_{SM} anomalies tend to decrease coherently. The years 1957 and 1993 have significant reductions in both P_{TC} and P_{SM} and are sorted in the T−S− type. One more interesting feature disclosed by Table 3 is that there are two major ways to significantly increase total rainfall in Taiwan (i.e., T+S− and T−S+), but only one major way to decrease it (i.e., T−S−). Also revealed is that the P_{TC} anomaly is larger in magnitude than the P_{SM} anomaly in 14 out of the 19 selected years. TC rainfall appears to play a more important role than seasonal monsoon rainfall in determining total rainfall variability in Taiwan.

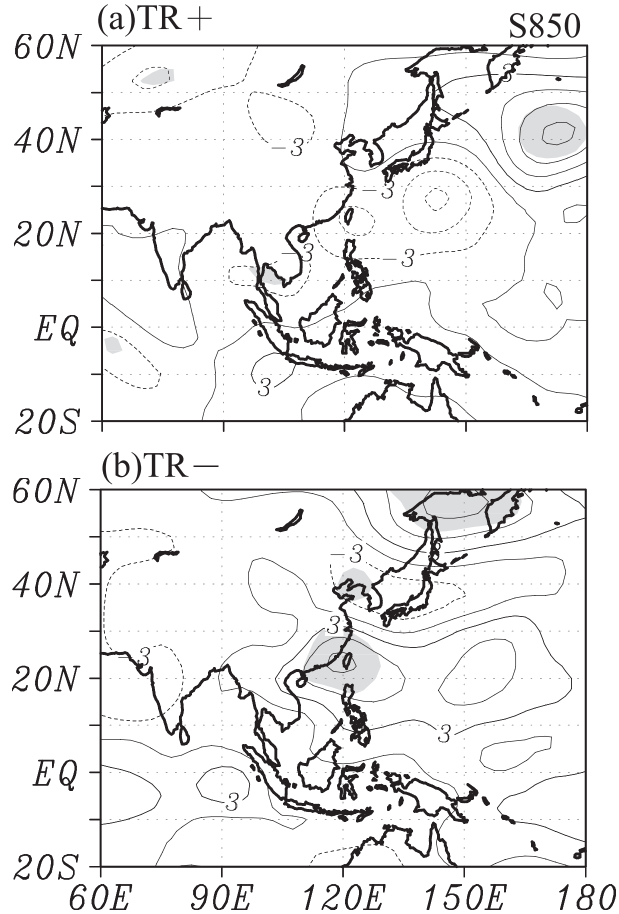

FIG. 11. As in Fig. 6, but for composite S850 anomalies of the (a) increased total rainfall (TR+) type and (b) decreased total rainfall (TR−) type. Member years of the TR+ and TR− types are listed in Table 3. Contour intervals are 3×10^5 m^2 s^{-1}, and anomalies significant at the 95% level are shaded.

For the large-scale pattern, composite S850 anomalies of the TR+ and TR− types are displayed in Fig. 11. The TR+ type characterizes an anomalous cyclone over the WNP, with one center overlying Taiwan and the other one to the southeast of Japan. However, this anomalous cyclone is weak in intensity and lacks statistical significance. This is because Taiwan lies beneath an anomalous cyclone in 6 yr of the TR+ type but beneath an anomalous anticyclone in 4 yr (see Table 3). Such a mixture lowers the statistical significance of anomalies in the composite analysis. For the TR− type, its composite S850 anomalies characterize a significant anomalous anticyclone elongated across the WNP and Taiwan. In fact, Taiwan is underlying an anomalous anticyclone in all 9 yr of the TR− type. The appearance of anomalous anticyclone suppresses P_{SM} in Taiwan by hindering vertical motion near its central region. It also enhances vertical wind shear over the tropical western

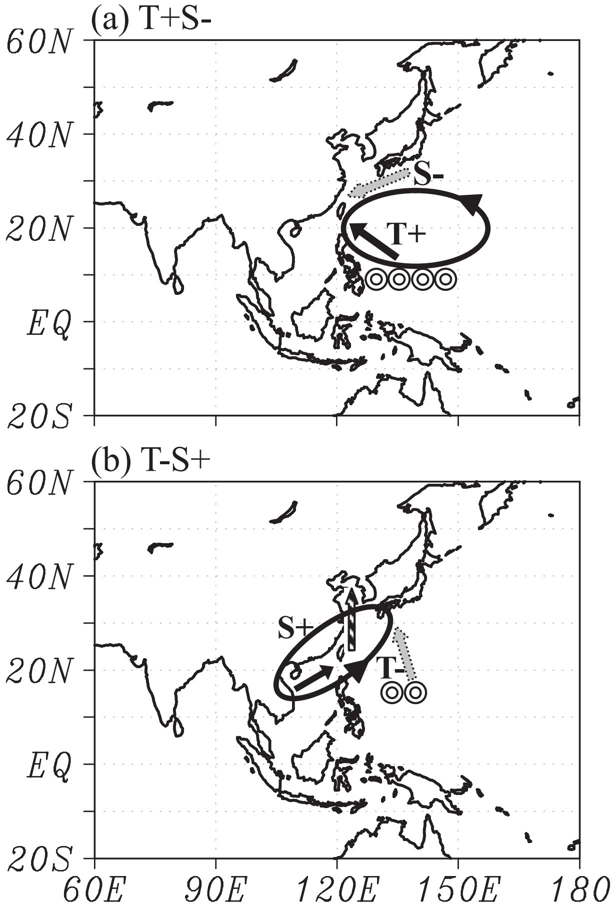

FIG. 12. Schematic diagrams for the major processes regulating rainfall variability in Taiwan: (a) the T+S− type and (b) the T−S+ type. In (a), decreased P_{SM} (S−) is caused by anomalous northeasterly water vapor fluxes (light arrow) and weak vertical motion over the western boundary of the anomalous cyclone. Increased P_{TC} (T+) concurs with more TC formation in the regions southeast of Taiwan (more ⊚ symbols) and mean southeasterly flows to steer TCs toward Taiwan (dark solid arrow). In (b), increased P_{SM} (S+) is induced by strong ascending motion (dark slashed arrow) and enhanced water vapor fluxes from the SCS into Taiwan (dark solid arrow) nearby the anomalous cyclone center. Decreased P_{TC} (T−) concurs with reduced TC formation (fewer ⊚ symbols) and mean southerly flows to guide TCs toward Japan and the North Pacific (light arrow).

Pacific to inhibit TC formation, which further leads to reduced TC frequency in Taiwan (e.g., Chen et al. 2005). Under these circumstances, both P_{SM} and P_{TC} decrease in Taiwan. Other single-index analyses are conducted for the variability types categorized by one SD of P_{TC} or P_{SM} alone. There are 7/11 yr in the deficient/abundant P_{TC} type (denoted as T−/T+ type), and 10/8 yr in the suppressed/enhanced P_{SM} type (denoted as S−/S+ type). Major composite $S850$ patterns (not shown) over the WNP and Taiwan are statistically insignificant (less than the 95% significance level) in the T−, S−, and S+ types due to a mixture of cyclonic and anticyclonic anomalies in individual member cases. On the contrary, the analyses with dual indexes in the present study obtain a uniform anomalous cyclone overlying Taiwan for all 13 yr of the T+S− and T−S+ types, resulting in statistical significance in their composite $S850$ anomalies (see Fig. 6). The earlier comparisons suggest that the use of dual indexes helps to better extract climate signals, and thus obtain more coherent and significant climate variability features.

8. Concluding remarks

Rainfall in Taiwan during the warmer half of the year is evidently affected by both the monsoon system and TC activity to exhibit noticeable interannual variability. The main purpose of this study is to examine how monsoons and TCs modulate interannual rainfall variability over Taiwan during July–September. The analysis period spans from 1950 to 2002. To examine the relative roles, rainfall in Taiwan is separated into two subcomponents: TC rainfall (P_{TC}) and seasonal monsoon rainfall (P_{SM}). Rainfall occurring in Taiwan during the days with a TC centering in a spatial zone close to Taiwan within 2.5° in longitude and latitude (19.5°–27.5°N, 117.5°–124.5°E) is defined as TC rainfall. Other than TC rainfall, the remaining contribution to rainfall is considered to be primarily induced by seasonal monsoon climate and thus referred to as seasonal monsoon rainfall.

Climatologically, P_{TC} and P_{SM} account for percentages of 47.5% and 52.5% of total rainfall, respectively, showing a comparable contribution to total rainfall. On an interannual time scale, P_{SM} and P_{TC} tend to vary inversely, with a simultaneous negative correlation (−0.46) between their 1950–2002 time series. They exhibit two major variability types: enhanced P_{TC} but suppressed P_{SM} (T+S−) and suppressed P_{TC} but enhanced P_{SM} (T−S+). Large-scale regulating processes for these two types are illustrated by schematic diagrams in Fig. 12. For the T+S− type, its salient feature is a low-level anomalous cyclone southeast of Taiwan. Its western boundary concurs with weakened vertical motion overlying Taiwan and anomalous northeasterly water vapor fluxes to reduce mean moisture supplies from the SCS into Taiwan, leading to deficient seasonal monsoon rainfall (S−). The anomalous cyclone leads to strong positive relative vorticity and ascending motion anomalies southeast of Taiwan, causing more TC formation there. The so-formed TCs are further steered by mean southeasterly flows to move toward Taiwan, resulting in increased TC frequency and TC rainfall in Taiwan (T+). The T−S+ type exhibits an anomalous cyclone with its centers displacing northwestward over Taiwan. It enhances seasonal monsoon rainfall in Taiwan (S+) via strengthened upward motion and water vapor fluxes from the SCS into Taiwan. Following the northwestward displacement of the anomalous cyclone, ascending motion and low-level relative vorticity anomalies become much weaker southeast of Taiwan to suppress TC formation there. Moreover, mean steering flows become southerly and drive TCs to recurve northward toward Japan and the North Pacific. Both TC frequency and TC rainfall thus decrease in Taiwan (T−).

Analyses of interannual rainfall variability are compared between categorizations by two rainfall subcomponents (P_{TC} and P_{SM}) and by total rainfall. It is shown that significant increases in total rainfall in Taiwan are attributable to an increase in either P_{TC} or P_{SM} but not both. Wet years, in aggregate, are a mixture of both T+S− and T−S+ type years. Their composite S850 anomalies become insignificant due to a lack of a uniform anomaly pattern. By contrast, analyses with dual indexes can extract more coherent climate signals. Their rainfall variability types are found to be regulated by relatively consistent large-scale processes.

The measurement of P_{TC} may be sensitive to the data quality of the JTWC best-track data. According to Chu et al. (2002), the post-1985 best-track data are of higher quality than previous data. We thus partition the data into two periods—1950–84 and 1985–2002—and compute the correlation coefficients between P_{TC} and P_{SM} time series for the two periods. The result is −0.45 for the former and −0.49 for the latter period. No evident difference occurs in the correlation coefficients. This suggests that a reverse phase relationship between P_{TC} and P_{SM} in Taiwan is a robust feature, which is not affected by the quality of the best-track data.

The approach of dual indexes provides a new perspective for studying and predicting interannual rainfall variability via separation of rainfall into TC- and monsoon-induced rainfall subcomponents. Our analyses illustrate TC- and monsoon-induced rainfall variability to be strongly sensitive to large-scale circulation anomalies. For example, a northwestward displacement of the anomalous S850 cyclone center may change rainfall variability in Taiwan from the T+S− type into the T−S+ type. These findings are potentially useful for improved regional climate prediction. Because the physical mechanisms that regulate the two rainfall subcomponents are different, it is necessary to predict TC and seasonal monsoon rainfall anomalies separately by building different statistical models. The current approach can take advantage of more coherent circulation patterns sorted by rainfall subcomponents compared with those sorted by a total rainfall index. As such, higher prediction skills may be obtained. The predicted subcomponents can be added together to make total rainfall predictions. It is anticipated that this indirect prediction approach may be more skillful than the direct prediction of total rainfall. Further studies are needed to evaluate practical skills of the two prediction approaches mentioned earlier. It is worth noting that there is also weakness associated with the current dual-index approach. As revealed by Tables 2 and 3, the dual-index approach results in more variability types but fewer member samples for each type. As a result, the composite result may lack statistical significance. Future observational and modeling studies are needed to reveal robust large-scale circulation signals associated with the different monsoon–TC rainfall types.

Acknowledgments. The authors thank the anonymous reviewers for their valuable comments, which helped improve the quality of this paper. This study was supported by the National Science Council, Taiwan, under NSC Grant 95-2111-M-022-001-MY3 and NSC Grant 98-2623-E-022-001-D. TL was supported by ONR Grant N000140810256 and NRL Grant N00173091G008 and by the International Pacific Research Center, which is sponsored by the Japan Agency for Marine-Earth Science and Technology (JAMSTEC), NASA (NNX07AG53G), and NOAA (NA17RJ1230).

REFERENCES

Bessafi, M., and M. C. Wheller, 2006: Modulation of south Indian Ocean tropical cyclones by the Madden–Julian oscillation and convectively coupled equatorial waves. *Mon. Wea. Rev.,* **134,** 638–656.

Chan, J. C. L., 2000: Tropical cyclone activity over the western North Pacific associated with El Niño and La Niña events. *J. Climate,* **13,** 2960–2972.

Chang, C.-P., and G. T.-J. Chen, 1995: Tropical circulation associated with southwest monsoon onset and westerly surges over the South China Sea. *Mon. Wea. Rev.,* **123,** 3254–3267.

——, Y. Zhang, and T. Li, 2000a: Interannual and interdecadal variations of the East Asian summer monsoon and tropical Pacific SSTs. Part I: Roles of subtropical ridge. *J. Climate,* **13,** 4310–4325.

——, ——, and ——, 2000b: Interannual and interdecadal variations of the East Asian summer monsoon and tropical Pacific SSTs. Part II: Meridional structure of the monsoon. *J. Climate,* **13,** 4326–4340.

Chen, C.-S., and Y.-L. Chen, 2003: The rainfall characteristics of Taiwan. *Mon. Wea. Rev.,* **131,** 1323–1341.

——, ——, C.-L. Liu, P.-L. Lin, and W.-C. Chen, 2007: Statistics of heavy rainfall occurrences in Taiwan. *Wea. Forecasting,* **22,** 981–1002.

Chen, G. T.-J., 1994: Large-scale circulation associated with the East Asian summer monsoon and the Mei-Yu over South China and Taiwan. *J. Meteor. Soc. Japan,* **72,** 959–983.

——, and C.-C. Yu, 1988: Study of low-level jet and extremely heavy rainfall over northern Taiwan in the mei-yu season. *Mon. Wea. Rev.,* **116,** 884–891.

Chen, J.-M., and H.-L. Fan, 2003: Interannual variability of the South China Sea summer rainfall and typhoon invading Taiwan (in Chinese). *Atmos. Sci.,* **31,** 221–238.
——, F.-C. Lu, S.-L. Kuo, and C.-F. Shih, 2005: Summer climate variability in Taiwan and associated large-scale processes. *J. Meteor. Soc. Japan,* **83,** 499–516.
——, T. Li, and C.-F. Shih, 2007: Fall persistence barrier of sea surface temperature in the South China Sea associated with ENSO. *J. Climate,* **20,** 158–172.
——, ——, and ——, 2008: Asymmetry of the El Niño-spring rainfall relationship in Taiwan. *J. Meteor. Soc. Japan,* **86,** 297–312.
——, J.-L. Chu, C.-F. Shih, and Y.-C. Tung, 2010: Interannual variability of circulation-rainfall relationship in Taiwan during the Mei-yu season. *Int. J. Climatol.,* in press, doi:10.1002/joc.2049.
Chen, T.-C., and J.-M. Chen, 1995: An observational study of the South China Sea monsoon during the 1979 summer: Onset and life cycle. *Mon. Wea. Rev.,* **123,** 2295–2318.
——, S.-P. Weng, N. Yamazaki, and S. Kiehne, 1998: Interannual variation in the tropical cyclone formation over the western North Pacific. *Mon. Wea. Rev.,* **126,** 1080–1090.
——, S.-Y. Wang, M.-C. Yen, and A. Clark, 2009: Impact of the intraseasonal variability of the western North Pacific large-scale circulation on tropical cyclone tracks. *Wea. Forecasting,* **24,** 646–666.
Chia, H.-H., and C. F. Ropelewski, 2002: The interannual variability in the genesis location of tropical cyclones in the northwest Pacific. *J. Climate,* **15,** 2934–2944.
Chou, C., J.-Y. Tu, and J.-Y. Yu, 2003: Interannual variability of the western North Pacific summer monsoon: Differences between ENSO and non-ENSO years. *J. Climate,* **16,** 2275–2287.
Chu, J.-H., C. R. Sampson, A. S. Levine, and E. Fukada, cited 2002: The Joint Typhoon Warning Center tropical cyclone best-tracks, 1945-2000. NRL Reference NRL/MR/7540-02-16. [Available online at http://metoph.nmci.navy.mil/jtwc/best_tracks/TC_bt_report.html.]
Ding, Y. H., 1994: *Monsoon Over China*. Kluwer Academic Publishers, 419 pp.
Fu, B., T. Li, M. Peng, and F. Weng, 2007: Analysis of tropical cyclone genesis in the western North Pacific for 2000 and 2001. *Wea. Forecasting,* **22,** 763–780.
Gross, J. M., 1991: The effect of shallow, medium and deep layer mean wind in the beta and advection model. Preprints, *19th Conf. on Hurricanes and Tropical Meteorology,* Miami, FL, Amer. Meteor. Soc., 104–106.
Hall, J. D., A. J. Matthews, and D. J. Karoly, 2001: The modulation of tropical cyclone activity in the Australian region by the Madden–Julian oscillation. *Mon. Wea. Rev.,* **129,** 2970–2982.
Harr, P. A., and R. L. Elsberry, 1991: Tropical cyclone track characteristics as a function of large-scale circulation anomalies. *Mon. Wea. Rev.,* **119,** 1448–1468.
——, and ——, 1995: Large-scale circulation variability over the tropical western North Pacific. Part I: Spatial patterns and tropical cyclone characteristics. *Mon. Wea. Rev.,* **123,** 1225–1246.
Ho, C.-H., J.-J. Baik, J.-H. Kim, and D.-Y. Gong, 2004: Interdecadal changes in summertime typhoon tracks. *J. Climate,* **17,** 1767–1776.
——, J.-H. Kim, H.-S. Kim, C.-H. Sui, and D.-Y. Gong, 2005: Possible influence of the Antarctic Oscillation on tropical cyclone activity in the western North Pacific. *J. Geophys. Res.,* **110,** D19104, doi:10.1029/2005JD005766.
Hoyos, C. D., and P. Webster, 2007: The role of intraseasonal variability in the nature of Asian monsoon precipitation. *J. Climate,* **20,** 4402–4424.
Hsu, H.-H., 2005: East Asian and western North Pacific summer monsoon region. *Intraseasonal Variability in the Atmosphere-Ocean System,* W. K. M. Lau and D. E. Waliser, Eds., Springer-Praxis, 65–98.
——, and C.-T. Chen, 2002: Observed and projected climate change in Taiwan. *Meteor. Atmos. Phys.,* **79,** 87–104.
Hsu, P.-C., C.-H. Tsou, W.-S. Kau, and H.-H. Hsu, 2005: Interannual variations of the intraseasonal oscillation during typhoon season over western Pacific (in Chinese). *Atmos. Sci.,* **33,** 29–48.
Huang, R., and Y. Wu, 1989: The influence of ENSO on the summer climate change in China and its mechanisms. *Adv. Atmos. Sci.,* **6,** 21–32.
Hung, C-w., H.-H. Hsu, and M.-M. Lu, 2004: Decadal oscillation of spring rain in northern Taiwan. *Geophys. Res. Lett.,* **31,** L22206, doi:10.1029/2004GL021344.
Jiang, H., and E. J. Zipser, 2010: Contribution of tropical cyclones to the global precipitation from eight seasons of TRMM data: Regional, seasonal, and interannual variations. *J. Climate,* **23,** 1526–1543.
Jiang, X., T. Li, and B. Wang, 2004: Structures and mechanisms of the northward propagating boreal summer intraseasonal oscillation. *J. Climate,* **17,** 1022–1039.
Jiang, Z., G. T.-J. Chen, and M.-C. Wu, 2003: Large-scale circulation patterns associated with heavy spring rain events over Taiwan in strong and non-ENSO years. *Mon. Wea. Rev.,* **131,** 1769–1782.
Kalnay, E., and Coauthors, 1996: The NCEP/NCAR 40-Year Reanalysis Project. *Bull. Amer. Meteor. Soc.,* **77,** 437–471.
Kang, I.-S., C.-H. Ho, Y.-K. Lim, and K.-M. Lau, 1999: Principal modes of climatological seasonal and intraseasonal variation of the Asian summer monsoon. *Mon. Wea. Rev.,* **127,** 322–340.
Kim, J.-H., C.-H. Ho, C.-H. Sui, and S. K. Park, 2005: Dipole structure of interannual variations in summertime tropical cyclone activities over East Asia. *J. Climate,* **18,** 5344–5356.
——, ——, H.-S. Kim, C.-H. Sui, and S. K. Park, 2008: Systematic variation of summertime tropical cyclone activity in the western North Pacific in relation to the Madden–Julian oscillation. *J. Climate,* **21,** 1171–1191.
Ko, K.-C., and H.-H. Hsu, 2009: ISO modulation on the submonthly wave pattern and recurving tropical cyclones in the tropical western North Pacific. *J. Climate,* **22,** 582–599.
Krishnamurthy, V., and J. Shukla, 2007: Intraseasonal and seasonally persisting patterns of Indian monsoon rainfall. *J. Climate,* **20,** 3–20.
Kubota, H., and B. Wang, 2009: How much do tropical cyclones affect seasonal and interannual rainfall variability over the western North Pacific? *J. Climate,* **22,** 5495–5510.
Lander, M., 1994: An exploratory analysis of the relationship between tropical storm formation in the western North Pacific and ENSO. *Mon. Wea. Rev.,* **122,** 636–651.
Lau, K.-M., G. J. Yang, and S. H. Shen, 1988: Seasonal and intraseasonal climatology of summer monsoon rainfall over East Asia. *Mon. Wea. Rev.,* **116,** 18–37.
Li, T., and B. Wang, 1994: The influence of sea surface temperature on the tropical intraseasonal oscillation: A numerical study. *Mon. Wea. Rev.,* **122,** 2349–2362.
——, and ——, 2005: A review on the western North Pacific monsoon: Synoptic-to-interannual variabilities. *Terr. Atmos. Oceanic Sci.,* **16,** 285–314.
Liebmann, B., H. H. Hendon, and J. D. Glick, 1994: The relationship between tropical cyclones of the western Pacific and Indian Oceans and the Madden-Julian oscillation. *J. Meteor. Soc. Japan,* **72,** 401–411.

Lim, Y.-K., K.-Y. Kim, and H.-S. Lee, 2002: Temporal and spatial evolution of the Asian summer monsoon in the seasonal cycle of synoptic fields. *J. Climate,* **15,** 3630–3644.

Liu, C.-M., 1996: *Weather and Climate in Taiwan* (in Chinese). Formosa Folkways Print, 366 pp.

Liu, Y., and Y. H. Ding, 1992: Influence of El Niño on weather and climate in China. *Acta Meteor. Sin.,* **6,** 117–131.

Lu, R., 2001: Interannual variability of the summertime North Pacific subtropical high and its relationship to atmospheric convection over the warm pool. *J. Meteor. Soc. Japan,* **79,** 771–783.

Madden, R. A., and P. R. Julian, 1971: Detection of a 40–50 day oscillation in the zonal wind in the tropical Pacific. *J. Atmos. Sci.,* **28,** 702–708.

Mao, J., and C. L. Chan, 2005: Intraseasonal variability of the South China Sea summer monsoon. *J. Climate,* **18,** 2388–2402.

McBride, J. J., 1995: Tropical cyclone formation. Global perspectives on tropical cyclones. Rep. TCP-38, WMO/TD-693, 63–105.

Parthasarathy, B., R. R. Kumar, and D. R. Kothawale, 1992: Indian summer monsoon rainfall indices, 1871-1990. *Meteor. Mag.,* **121,** 174–186.

Sui, C.-H., P.-H. Chung, and T. Li, 2007: Interannual and interdecadal variability of the summertime western North Pacific subtropical high. *Geophys. Res. Lett.,* **31,** L11701, doi:10.1029/2006GL029204.

Wang, B., 1994: Climatic regimes of tropical convection and rainfall. *J. Climate,* **7,** 1109–1118.

——, and X. Xie, 1997: A model for the boreal summer intraseasonal oscillation. *J. Atmos. Sci.,* **54,** 72–86.

——, and Z. Fan, 1999: Choice of South Asian summer monsoon indices. *Bull. Amer. Meteor. Soc.,* **80,** 629–638.

——, and J. C. L. Chan, 2002: How strong ENSO events affect tropical storm activity over the western North Pacific. *J. Climate,* **15,** 1643–1658.

——, and LinHo, 2002: Rainy season of the Asian–Pacific summer monsoon. *J. Climate,* **15,** 386–398.

——, and Q. Zhang, 2002: Pacific–East Asian teleconnection. Part II: How the Philippine Sea anomalous anticyclone is established during El Niño development. *J. Climate,* **15,** 3252–3265.

——, and T. Li, 2004: East Asian monsoon–ENSO interactions. *East Asian Monsoon,* C.-P. Chang, Ed., Series on Meteorology of East Asia, Vol. 2, World Scientific, 177–212.

——, R. Wu, and X. Fu, 2000: Pacific–East Asian teleconnection: How does ENSO affect East Asian climate. *J. Climate,* **13,** 1517–1536.

——, ——, and K.-M. Lau, 2001: Interannual variability of the Asian summer monsoon: Contrasts between the Indian and the western North Pacific–East Asian monsoons. *J. Climate,* **14,** 4073–4090.

——, ——, and T. Li, 2003: Atmosphere–warm ocean interaction and its impact on Asian–Australian monsoon variation. *J. Climate,* **16,** 1195–1211.

Wang, S.-Y., and T.-C. Chen, 2008: Measuring East Asian summer monsoon rainfall contributions by different weather systems over Taiwan. *J. Appl. Meteor. Climatol.,* **47,** 2068–2080.

Wu, B., T. Zhou, and T. Li, 2009: Seasonally evolving dominant interannual variability modes of East Asian climate. *J. Climate,* **22,** 2992–3005.

——, T. Li, and T. Zhou, 2010: Relative contributions of the Indian Ocean and local SST anomalies to the maintenance of the western North Pacific anomalous anticyclone during El Niño decaying summer. *J. Climate,* **23,** 2974–2986.

Wu, M. L. C., S. Schubert, and N. E. Huang, 1999: The development of the South Asian summer monsoon and the intraseasonal oscillation. *J. Climate,* **12,** 2054–2075.

Wu, R., 2002: Processes for the northeastward advance of the summer monsoon over the western North Pacific. *J. Meteor. Soc. Japan,* **80,** 67–83.

Xie, P., and P. A. Arkin, 1997: Global precipitation: A 17-year monthly analysis based on gauge observations, satellite estimates, and numerical model outputs. *Bull. Amer. Meteor. Soc.,* **78,** 2539–2558.

Yoo, S.-H., C.-H. Ho, S. Yang, H.-J. Choi, and J.-G. Jhun, 2004: Influences of tropical western and extratropical Pacific SST on East and Southeast Asian climate in the summers of 1993–94. *J. Climate,* **17,** 2673–2687.